ATMOSPHERIC ENVIRONMENT: X 12 (2021) 100136

Contents lists available at ScienceDirect

Atmospheric Environment: X

journal homepage: www.journals.elsevier.com/atmospheric-environment-x

Isoprene emission characteristics of tall and dwarf bamboos

Ting-Wei Chang [a,*], Yoshiko Kosugi [a], Motonori Okumura [b], Linjie Jiao [a], Siyu Chen [a], Dingkang Xu [a], Zhining Liu [a], Shozo Shibata [a], Ken-Hui Chang [c]

[a] Graduate School of Agriculture, Kyoto University, Kyoto 606-8502, Japan
[b] Research Institute of Environment, Agriculture and Fisheries, Osaka Prefecture, Habikino, Osaka 583-0862, Japan
[c] Department of Safety, Health and Environmental Engineering, National Yunlin University of Science and Technology, Yunlin 64002 Taiwan

ARTICLE INFO

Keywords:
Isoprene
Leaf mass per area
Electron transport rate
Bambusoideae
Phyllostachys
Semiarundinaria
Pleioblastus
Sasa
Sasaella

Considerable isoprene emissions from several bamboo species have been reported. However, bamboos are highly diverse in taxonomy and have different niches or habitats among species, and the present investigation might be insufficient to conclude a representative isoprene emission trait for bamboos. In this study, isoprene flux, leaf mass per area (LMA), photosynthetic rate, and electron transport rate (ETR) observations were conducted for 18 species within five genera of bamboo species, which include different growth types (tall and dwarf) and climates of the region of origin (temperate, warm-temperate, and subtropical). As a result, we observed that dwarf bamboos exhibited very low or no emission; in contrast, tall bamboos demonstrated considerable isoprene emission fluxes mainly in August and September 2019 at temperatures greater than 30 °C. For tall bamboos, isoprene emission fluxes, photosynthetic rate, and ETR in area-based units were correlated with LMA. To exclude the systematic correlation among isoprene emission flux, photosynthetic rate, and ETR, correlations among the observations of mass-based units were also tested, and the results demonstrated significant positive correlations. The distinction in isoprene emission traits between tall and dwarf bamboos was independent of LMA, photosynthetic rate, and ETR, as there was no difference between them. This implies that the distinction in isoprene emission was caused by genetic differences. The low emission of isoprene from the dwarf species is reasonable because dwarf bamboos usually grow in areas with relatively low heat stress and low light where the production of isoprene could be futile due to carbon loss. This study suggests separating the two bamboo types into different functional types of isoprene emissions.

Abstract.

1. Introduction

Isoprene is one of the major biogenic volatile organic compounds (BVOCs) in the atmosphere, with an estimated emission of approximately 400–700 Tg of carbon annually, and it accounts for approximately 50–70 % of the total terrestrial BVOC emissions (Guenther et al., 2006, 2012; Sindelarova et al., 2014). This emission is comparable in magnitude to the global methane emission, which was estimated at 410–660 Tg of carbon per year, from 2008 to 2017 (Saunois et al., 2020). Isoprene is known to affect atmospheric chemistry. BVOCs are estimated to be the largest source of secondary organic aerosol (SOA) mass on a global scale, ranging from 12 to 70 Tg per year (Kanakidou et al., 2005). As the largest BVOC, isoprene could be a major precursor for the formation of SOAs through photooxidation under low NO_x concentrations in the atmosphere or with hydrogen peroxide under acid-catalyzed oxidation (Claeys et al., 2004a; b). A chamber study on the photooxidation of isoprene demonstrated that the SOA yield rates could be 1–2 % at high NO_x levels and approximately 3 % at low NO_x levels (Kroll et al., 2005, 2006). Furthermore, isoprene and its oxidation products (methyl vinyl ketone and methacrolein) could react with NO_x to form ozone in the troposphere (Kamens et al., 1982; Paulson et al., 1992; Paulson and Seinfeld, 1992; Teng et al., 2017). This effect has been recorded in urban green environments that are highly abundant in both isoprene and NO_x, which potentially worsen the air quality (Biesenthal et al., 1997; Dreyfus et al., 2002; Duane et al., 2002; Pang et al., 2009; Geng et al., 2011; Fierravanti et al., 2017). Non-methane volatile

* Corresponding author. Division of Environmental Science and Technology, Graduate School of Agriculture, Kyoto University, Kitashirakawa Oiwake-cho, Sakyo-ku Kyoto 606-8502, Japan.
E-mail addresses: tingwei.chang.85c@st.kyoto-u.ac.jp (T.-W. Chang), kosugi.yoshiko.4x@kyoto-u.ac.jp (Y. Kosugi), OkumuraM@mbox.kannousuiken-osaka.or.jp (M. Okumura), jiao.linjie.66x@st.kyoto-u.ac.jp (L. Jiao), chen.siyu.55x@st.kyoto-u.ac.jp (S. Chen), xu.dingkang.74x@st.kyoto-u.ac.jp (D. Xu), liu.zhining.86m@st.kyoto-u.ac.jp (Z. Liu), sho@kais.kyoto-u.ac.jp (S. Shibata), ken@airlab.yuntech.edu.tw (K.-H. Chang).

https://doi.org/10.1016/j.aeaoa.2021.100136
Received 5 April 2021; Received in revised form 3 October 2021; Accepted 13 October 2021
Available online 14 October 2021

hydrocarbons, including isoprene, also have the potential to prolong methane life span in the atmosphere by reducing radicals, consequently leading to global warming; however, this depends on the VOC and NO_x ratio, as isoprene-induced radicals can also shorten the life span of methane (Poisson et al., 2000; Spivakovsky et al., 2000; Collins et al., 2002; Pike and Young 2009; Archibald et al., 2011).

Bamboos are important components of ecosystems, accounting for 3.2 % (36.8 million hectares) of global forest area and occupy 23.6 million hectares in Asia (Lobovikov et al., 2007). Several bamboo species, regardless of growth type, have been reported to expand and invade multiple regions (Okutomi et al., 1996; Torii, 2003; Kudo et al., 2011; Takada et al., 2012). Bamboos are plant species under the *Bambusoideae* subfamily, comprising over 1500 species with highly diverse growing traits (Kleinhenz and Midmore, 2001; Clark et al., 2015). In Japan, bamboos include two major subtribe classifications: *Arundinariinae* and *Shibataeinae* subtribes. *Shibataeinae* includes species with tall culms, and *Arundinariinae* is composed of both tall and dwarf bamboos. *Shibataeinae* is believed to have originated from tropical, subtropical or warm-temperate climate regions in China, then imported and adapted in Japan, and *Arundinariinae* originated from warm-temperate to temperate regions in Japan. Nevertheless, bamboo species exhibit a diversity in distribution of habitats; furthermore, even within the same genus, different species might originate from different climates (e.g., *Pleioblastus hindsii*, originated from subtropical regions; *Pleioblastus chino*, originated from temperate regions), which could imply different degrees of heat stress. In addition to climate, a major difference in niche can be observed between the two growth types of bamboos, where dwarf bamboos usually grow in more shaded environments than the tall species.

Evidence has shown that isoprene production in plants can promote tolerance to multiple stresses, such as heat, oxidation, and over-irradiance, which can damage cellular membranes or chloroplast membranes in leaves (Siwko et al., 2007; Loreto and Velikova, 2001; Way et al., 2011). However, isoprene emission can also be a cost to the plant in terms of both carbon and energy loss, which is a disadvantage in plant growth (Sharkey and Loreto, 1993). This implies and manifests in different isoprene emission traits of different plant species for fitness to environmental conditions (Sharkey and Loreto, 1993; Monson et al., 2013). Previous studies have revealed that plants produce dimethylallyl pyrophosphate (DMAPP) through 2-C-methyl-D-erythritol 4-phosphate/1-deoxy-D-xylulose 5-phosphate (MEP/DOXP) pathways and convert it to isoprene in the cells of the thylakoid membrane on the stromal side of chloroplasts (Wildermuth and Fall, 1996, 1998; Sasaki et al., 2005). The catalytic reaction of the isoprene synthesis enzyme, isoprene synthase (IspS), which converts DMAPP to isoprene, is required and plays a role in regulating the production rate of isoprene (Silver and Fall 1991; Sasaki et al., 2005; Oku et al., 2014). The IspS gene is absent in several plant species and this causes non-emission of isoprene from these species (Monson et al., 2013). A previous study demonstrated that isoprene emission ability could vary among species within a genus (e.g., *Quercus* spp., Tani and Kawawata, 2008).

Although the increasing numbers in the area of bamboos, only 2 out of 17 species (i.e., *Phyllostachys pubescens* and *Pleioblastus hindsii*; Chang et al., 2012) are assigned emission flux values based on the observations available in "MEGAN2019b vegetation type EF" (https://bai.ess.uci.edu/megan/data-and-code#h.p_UD2ckP0JM58D), the current default database of MEGANv3.1, while the remaining 15 species were assigned assumed values. Other studies on isoprene emission flux from bamboo leaves (e.g., Okumura et al., 2018; Chang et al., 2019) recorded the emission fluxes for a limited number of leaves. However, isoprene emission could also be highly diverse among bamboo species (Okumura et al., 2018). Therefore, it is necessary to observe isoprene emissions from multiple bamboo species for providing realistic emission inventory for better estimation of BVOCs emissions from bamboo species.

At the leaf scale, the concentration of chloroplasts could affect the isoprene emission rate because isoprene is produced in chloroplasts; higher isoprene emission fluxes could be expected in thicker leaves. As a related factor to leaf thickness (Liakoura et al., 2009), Harley et al. (1997) reported a relationship between isoprene emission flux and leaf mass per area (LMA) while using area-based units of isoprene emission flux. In addition, according to the process base of isoprene production, the isoprene product is constrained to the DMAPP pool size, which incorporates pyruvate and glyceraldehyde 3-phosphate into the 5-carbon skeleton to form DMAPP (Wiberley et al., 2009; Vickers et al., 2011; Monson et al., 2012; Schwender et al., 1997; Rohmer, 1999; Lichtenthaler, 1999). The pool size of DMAPP is highly related to photosynthetic chemistry, where the substrate, reducing equivalent, and energy equivalent are acquired and limited by the electron transport rate (ETR) (Brüggemann and Schnitzler, 2002; Rosenstiel et al., 2002; Rasulov et al., 2009, 2018). Thus, there is a need to discriminate between the effect of LMA and photosynthetic traits when comparing isoprene emission genotypes across multiple species.

To clarify (1) whether there is a distinction of isoprene emission traits among bamboo species and if so, (2) whether the differences could be explained by differences in LMA or caused by photosynthetic traits such as the photosynthetic rate or ETR, this study measured isoprene emission fluxes and other factors of 18 species of bamboos within five genera, including dwarf and tall bamboo types; part of the genera includes species originating from different climates.

2. Materials and methods

2.1. Site and subject species of bamboo

The field work was conducted in bamboo specimen plots located at Kamigamo experimental station, Kyoto, Japan (35° 04′ N, 135° 46' E), with an annual temperature of 14.6 °C and annual precipitation of 1582 mm. The bamboos were grown by species, separately in concrete plots. This study selected the following 18 species within five genera as subjects: *Phyllostachys makinoi*, *Phyllostachys aurea*, *Phyllostachys bambusoides*, *Phyllostachys pubescens*, *Phyllostachys nigra* f. henonis, *Semiarundinaria fastuosa*, *Semiarundinaria yashadake*, *Semiarundinaria fortis*, *Semiarundinaria kagamiana*, *Pleioblastus hindsii*, *Pleioblastus linearis*, *Pleioblastus simonii*, *Pleioblastus chino*, *Sasa tsuboiana*, *Sasa veitchii*, *Sasa chartacea*, *Sasaella ramosa*, *Sasaella hortensis (Phyllostachys*, *Semiarundinaria*, *Pleioblastus*, *Sasa*, and *Sasaella* are hereinafter abbreviated as *P.*, *Se.*, *Pl.*, *S.*, and *Sa.*, respectively). Among them, *Phyllostachys* spp., *Semiarundinaria* spp., and *Pleioblastus* spp. are tall species, whereas *Sasa* spp. and *Sasaella* spp. are dwarf species. We categorize the 18 species into three classifications corresponding to their climate of origins: temperate area (TE) includes *Se. kagamiana*, *Pl. chino* and *S. chartacea*; warm-temperate area (WT) includes *P. bambusoides*, *P. pubescens*, *P. nigra f. henonis*, *Se.fastuosa*, *Se. yashadake*, *Se. fortis*, *Pl. simonii*, *S. tsuboiana*, *S. veitchii*, *Sa. ramosa* and *Sa. hortensis*; subtropical area (ST) includes *P. mokinoi*, *P. aurea*, *Pl. hindsii* and *Pl. linearis*. Noted that bamboos gradually defoliate at around January and begins to emerge leaf sprouts at around April and May. Isoprene measurements for some of the species (i.e., *Pl. chino*, *S. chartacea* and *Sa. ramosa*) in May 2020 were observed from new leaves due to die out of old leaf. For other species, old leaves of the 2019 season were observed until May 2020. Basing on our observations made from April 2019 to June 2020, most of the species used in this study share a similar leaf life cycle, whereby leaves usually emerge in April or May and fall after approximately 12–14 months. Only two species showed exceptions; one was *P. nigra* f. *henonis*, where the species underwent a synchronous flowering event in October 2019 then died out at about June 2020. The other was *P. pubescens*, which did not emerge any new leaf in 2020 spring and kept most of the leaves to second year. This two-year leaf lifespan of *P. pubescens* was also reported by previous study (Li et al., 1998a,b).

2.2. Field sampling

The measurements were conducted monthly from August 2019 to May 2020 (August 2–5, 2019; September 12–18, 2019; October 15–20, 2019; November 13–17, 2019; December 14–16, 2019; January 11–13, 2020; February 24–26, 2020; March 15–20, 2020; April 19–25, 2020; May 17–24, 2020). Each month, measurements were conducted on three leaves of each species. Leaves at or near the top of the culm, which was exposed to full sunlight with no obvious damage or least damage, were chosen for the measurements. A modified portable photosynthetic measuring system (LI-6400, Li-Cor Inc., Lincoln, NE, USA) was used to measure the photosynthetic rate, leaf temperature (T_L, °C), ETR, and isoprene collection. A fluorescence cuvette (LI-6400-40) was used during the ETR measurement. Isoprene collection was achieved with a slight modification of the air path between the leaf cuvette of LI-6400 and its infrared gas analyzer (IRGA) by adding a T-junction made of Teflon that divided the airpath into two channels. The setup of the modification is showed in Fig. 1. One of the channels was connected to the IRGA and the other channel was plugged to a glass tube filled with 250 mg Tenax-TA 60/80 mesh (GL Science Inc., Tokyo, Japan). A granular filter filled with activated charcoal was connected to the air inlet of the LI-6400 system to supply VOC-free air. Three steps were performed during each measurement of every leaf. First, the leaf was clapped by the leaf cuvette with controls on irradiance (1000 μmol m^{-2} s^{-1} of photosynthetic photon density flux, PPFD), and also on T_L for each monthly measurement campaigns from September to December 2019, where stable T_L were supplied to 30, 25, 20, and 10 °C respectively from September to December 2019 which were close to the ambient temperature corresponding to each month with an LED cuvette (LI-6400-02B, Li-Cor Inc.). We also attempted to manipulate T_L into 30 °C August 2019, however, the strong heat from sunlight caused a major influence on T_L among measurements. T_L of the measurements from January to May 2020 was not controlled and were close to ambient temperatures. During this step, the photosynthetic rate was measured without connecting the adsorbent tubes into the system. The photosynthetic rates were calculated in area-based form (A_{Area}, μmol m^{-2} s^{-1}) and mass-based form (A_{Mass}, μmol g^{-1} s^{-1}) using the following equations:

$$A_{Area} = A_{Origin} \cdot R_{Cuvette} / R_{Origin} \quad (1)$$

$$A_{Mass} = A_{Area} \cdot R_{Leaf} / M_{Leaf} \quad (2)$$

where A_{Origin} (μmol m^{-2} s^{-1}) is the measured value of the photosynthetic rate with the default leaf area (R_{Origin}) set at 6 cm^2, $R_{Cuvette}$ (cm^2) is the actual in-cuvette leaf area, R_{Leaf} (cm^2) and M_{Leaf} (g) is the whole leaf area and dry mass of the measured leaf, respectively.

After approximately 5 min to stabilize the isoprene concentration in the cuvette in the first step, next, an adsorbent tube was plugged into the T-junction channel on one side, and a micropump (MP-Σ30NII, SIBATA Inc., Tokyo, Japan) on the other side. The micropump was set at a rate of 150 mL min^{-1} to draw out the air from the cuvette for 400 s. Air (1 L) was passed through the adsorbent tube to trap the VOC component, including isoprene. After VOC collection, the adsorbent tube was immediately stored at a temperature of approximately 5 °C.

The final step of field sampling was to measure the ETR of the leaf using the fluorescence method. During this step, a standard light set at 1500 μmol m^{-2} s^{-1} of PPFD with 10 % blue light was supplied to the leaf, and the steady state fluorescence (F_S, μmol m^{-2} s^{-1}) was recorded when it stabilized. A 1-s light pulse with over 7000 μmol m^{-2} s^{-1} was then applied to acquire the maximum fluorescence (F_m, μmol m^{-2} s^{-1}). Area- and mass-based ETRs (ETR_{Area}, μmol m^{-2} s^{-1}; ETR_{Mass}, μmol g^{-1} s^{-1}) were calculated using the following equations:

$$ETR_{Area} = ((F_m - F_S) / F_m) \cdot L \cdot Q \cdot \alpha_{Leaf} \quad (3)$$

$$ETR_{Mass} = E_{Area} \cdot R_{Leaf} / M_{Leaf} \quad (4)$$

where L is the PPFD of standard light (1500 μmol m^{-2} s^{-1}), Q is the fraction of absorbed quanta used by photosystem II (assumed to be 0.5), and α_{Leaf} is the leaf absorptance (assumed to be 0.84).

2.3. Quantifying the isoprene emission flux

After the field measurements, the measured leaves and the adsorbent tubes were collected in the laboratory for analysis. The leaves were scanned before deformation then dried at 60 °C for 72 h to acquire R_{Leaf}, $R_{Cuvette}$, M_{Leaf}, and LMA.

To determine the isoprene concentration ($C_{Isoprene}$), isoprene content in the adsorbent tube was desorbed and re-trapped with a preconcentrator (Model 7100A, Entech Instruments Inc., CA, USA), and then introduced into a gas chromatography system with a mass spectrometer (HP6890, Agilent Technologies Inc., CA, USA) for identification and quantification. Area-based isoprene emission flux (I_{Area}, nmol m^{-2} s^{-1}) and mass-based isoprene emission flux (I_{Mass}, nmol g^{-1} s^{-1}) were calculated as follows:

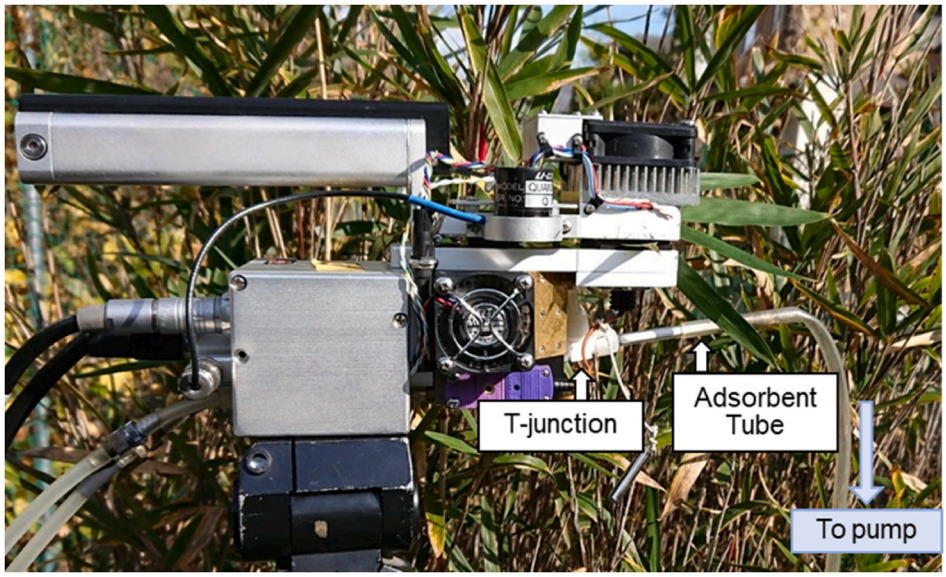

Fig. 1. Photo of LI-6400 cuvette during isoprene collection.

$$I_{Area} = C_{Isoprene} \cdot V / R_{Cuvette} \quad (6)$$

$$I_{Mass} = I_{Area} \cdot R_{Leaf} / M_{Leaf} \quad (7)$$

where V (μmol s^{-1}) is the flow velocity of LI-6400 air inflow.

3. Results

3.1. Isoprene emission fluxes of 18 species of bamboo from August 2019 to May 2020

The results of the measurement of isoprene emission from the subject bamboo species indicated a large range of I_{Area} (from 0 to 50.21 nmol m^{-2} s^{-1}). All species were found to emit isoprene in August 2019 and the emission gradually decreased or ceased from September 2019 to February 2020, before slowly increasing from March to May 2020. Noted that isoprene measurements for *Pl. chino*, *S. chartacea* and *Sa. ramosa* in May 2020 were observed from new leaves. The variation in isoprene emission fluxes generally corresponded with the fluctuation of leaf temperature; August 2019 had the highest leaf temperatures (30–35 °C) and January 2020 had the lowest leaf temperatures (~5 °C) (Table 1a; Table 1b).

A large difference in the relationship between isoprene emission and leaf temperature in each genus was recorded between the tall species (*Phyllostachys*, *Semiarundinaria,* and *Pleioblastus* spp.) and the dwarf species (*Sasa* and *Sasaella* spp.). The tall species exhibited large isoprene emission fluxes, which were mainly distributed in a leaf temperature range of 25–35 °C; whereas the dwarf species exhibited very low or no isoprene emission at all leaf temperatures (Fig. 2).

Since the major difference in isoprene emissions among the bamboo species was recorded in August and September 2019, the averaged I_{Area} and T_L of each species in August and September 2019 are plotted in Fig. 3. In August 2019, nine out of thirteen tall bamboo species exhibited isoprene emission fluxes larger than 20 nmol m^{-2} s^{-1} regardless of subtribe (*P. makinoi*, *P. pubescens*, *Se. yashadake*, *Se. fortis*, *Se. kagamiana*, *Pl. hindsii*, *Pl. linearis*, *Pl. simonii* and *Pl. chino*), however, none of the dwarf species demonstrated area-based emission fluxes larger than 10 nmol m^{-2} s^{-1}. On average, tall species demonstrated higher isoprene emission fluxes (August 2019: 25.24±12.71 nmol m^{-2} s^{-1}; September 2019: 11.37±4.66 nmol m^{-2} s^{-1}) compared to those of the dwarf species (August 2019: 1.96±2.80 nmol m^{-2} s^{-1}; September 2019: 0.34±0.60 nmol m^{-2} s^{-1}).

Moreover, when the isoprene emission fluxes were compared based on the climate of the region of origin, no significant difference in I_{Area} was observed among different climatic origins for both tall and dwarf species during August and September (Table 2).

A decrease in both isoprene emission and leaf temperature was observed in most of the species from August to September. However, this decrease was not proportional to the change in leaf temperature. For instance, *P. makinoi* demonstrated a 64 % decrease in isoprene emission flux without a large difference in leaf temperature; in contrast, *Pl. chino* exhibited no significant change in isoprene emission flux, while a large difference in leaf temperature was observed.

3.2. Relationship between LMA and isoprene emission flux

Positive relationships were observed between area-based isoprene emission flux and LMA of the tall species when the monthly linear relationship was evaluated separately (Table 3a). The tall species exhibited slopes of 0.574 and 0.238 in August and September 2019, respectively; no linear relationship between area-based isoprene emission flux and LMA was observed in the dwarf species (Fig. 4). Although there was no significant difference in LMA between the dwarf species and the tall species (Table 3b), the isoprene emission of the dwarf species was lower than that of the tall species under any degree of LMA.

3.3. Relationship between photosynthetic traits and isoprene emission flux

In August and September 2019, the range of ETR_{Area} observation for the tall species and dwarf species were 30–160 μmol m^{-2} s^{-1} and 60–150 μmol m^{-2} s^{-1}, respectively, and most of the species demonstrated lower ETR_{Area} in September 2019 regardless of their growth types (Table 4). No significant differences were recorded between the tall species and dwarf species. Linear relationships between isoprene emission flux and ETR_{Area} were shown in the observations including those during August and September 2019 for the tall species; even more definitive relationships could be recorded if monthly observations were separately evaluated for the tall species, where R^2 in August and September 2019 were up to 0.378 and 0.542, respectively, and both of the correlations relationships were significant according to the analysis of *t*-test (p-value < 0.01) (Table 3a).

Since both the measurement of I_{Area} and ETR_{Area} in the area-based

Table 1a
Area-based isoprene emission flux and leaf temperature in each month from August 2019 to December 2020 of 18 bamboo species. The values are represented in mean ± standard deviation with three measurements.

Species	August 2019		September 2019		October 2019		November 2019		December 2019	
	I_{Area} (nmol m^{-2} s^{-1})	T_L (°C)	I_{Area} (nmol m^{-2} s^{-1})	T_L (°C)	I_{Area} (nmol m^{-2} s^{-1})	T_L (°C)	I_{Area} (nmol m^{-2} s^{-1})	T_L (°C)	I_{Area} (nmol m^{-2} s^{-1})	T_L (°C)
P. makinoi	36.8±12.3	30.3±0.5	13.3±6.4	30.0±0.1	3.3±0.5	24.9±0.0	7.7±1.5	19.9±0.0	3.8±0.4	10.0±0.1
P. aurea	14.9±5.7	30.7±0.7	11.3±2.6	29.9±0.0	4.0±1.2	25.0±0.0	7.7±1.1	19.9±0.0	3.9±0.2	9.9±0.0
P. bambusoides	17.5±2.1	30.2±0.5	6.3±1.2	30.0±0.0	1.5±0.3	24.9±0.0	5.7±2.6	20.0±0.0	10.0±2.8	10.0±0.0
P. pubescens	25.6±8.9	31.4±1.0	12.1±3.2	30.0±0.0	1.4±1.1	25.0±0.0	2.2±0.3	20.0±0.1	4.3±0.2	10.0±0.0
P. nigra f. henonis	4.9±3.7	30.2±0.3	6.9±1.7	30.0±0.0	0.9±0.1	24.7±0.1	0.4±0.6	20.0±0.1	n.d.	10.0±0.0
Se. fastuosa	14.2±3.6	30.8±0.2	6.2±0.8	30.0±0.0	0.8±0.1	24.8±0.1	1.5±0.3	19.8±0.1	n.d.	10.0±0.0
Se. yashadake	29.5±15.9	31.6±0.3	10.3±1.4	30.0±0.0	1.6±0.5	24.9±0.0	1.0±0.4	19.9±0.0	n.d.	10.0±0.0
Se. fortis	21.6±5.5	31.5±0.3	14.0±3.7	29.9±0.0	1.8±0.6	24.8±0.0	1.5±0.2	19.6±0.2	2.2±1.9	10.0±0.0
Se. kagamiana	23.5±5.8	31.7±0.3	9.8±3.1	30.0±0.0	1.2±0.2	24.8±0.1	0.9±0.1	19.9±0.0	0.7±1.2	10.0±0.0
Pl. hindsii	30.0±2.2	32.0±1.0	16.7±1.4	30.0±0.1	1.0±0.9	24.8±0.0	n.d.	19.3±0.2	n.d.	9.9±0.0
Pl. linearis	42.7±6.1	34.0±0.6	7.9±4.6	30.0±0.0	0.3±0.5	23.8±0.6	n.d.	19.8±0.2	n.d.	9.7±0.0
Pl. simonii	43.0±8.8	33.2±0.5	15.7±1.4	29.9±0.0	2.3±0.3	24.9±0.1	n.d.	19.9±0.0	n.d.	10.0±0.0
Pl. chino	24.0±7.9	33.5±0.2	18.3±2.4	29.9±0.0	2.6±0.3	24.9±0.0	n.d.	20.0±0.0	n.d.	9.9±0.0
S. tsuboiana	7.0±3.1	32.4±1.3	0.7±0.7	29.9±0.0	0.3±0.3	25.0±0.2	n.d.	19.7±0.2	n.d.	9.9±0.0
S. veitchii	0.2±0.2	30.4±0.4	n.d.	30.0±0.0	n.d.	25.0±0.2	n.d.	19.9±0.0	n.d.	9.7±0.0
S. chartacea	1.4±0.2	32.5±1.5	1.0±0.9	30.1±0.3	0.1±0.1	24.9±0.0	n.d.	19.9±0.0	n.d.	9.9±0.0
Sa. ramosa	0.6±0.2	31.1±0.2	n.d.	29.8±0.2	n.d.	24.7±0.0	n.d.	20.0±0.0	n.d.	9.9±0.0
Sa. hortensis	0.5±0.2	34.1±1.0	n.d.	30.0±0.1	n.d.	24.7±0.0	n.d.	20.0±0.0	n.d.	9.9±0.0

n.d.: No detection.

Table 1b
Area-based isoprene emission flux and leaf temperature in each month from January to May 2020 of 18 bamboo species. The values are represented in mean ± standard deviation with three measurements.

Species	January 2020		February 2020		March 2020		April 2020		May 2020	
	I_{Area} (nmol m^{-2} s^{-1})	T_L (°C)	I_{Area} (nmol m^{-2} s^{-1})	T_L (°C)	I_{Area} (nmol m^{-2} s^{-1})	T_L (°C)	I_{Area} (nmol m^{-2} s^{-1})	T_L (°C)	I_{Area} (nmol m^{-2} s^{-1})	T_L (°C)
P. makinoi	0.4±0.7	5.2±0.2	0.1±0.1	10.9±0.0	0.1±0.1	15.4±0.3	0.05±0.01	12.9±0.4	0.04±0.01	25.9±0.9
P. aurea	n.d.	5.2±0.1	0.1±0.0	11.0±0.0	0.1±0.0	12.9±0.5	0.1±0.1	14.3±0.3	1.8±3.1	30.0±1.0
P. bambusoides	1.0±0.0	5.5±0.5	0.1±0.0	11.0±0.0	0.4±0.2	14.8±0.1	1.0±0.1	14.5±0.5	6.2±3.5	26.8±1.6
P. pubescens	n.d.	6.1±0.0	0.03±0.03	11.0±0.0	0.1±0.0	10.7±1.3	0.2±0.1	15.6±1.5	2.4±0.4	31.2±0.5
P. nigra f. henonis	n.d.	5.3±0.0	n.d.	11.0±0.0	0.1±0.1	14.5±0.1	n.d.	15.7±0.1	1.2±2.2	25.1±0.8
Se. fastuosa	n.d.	5.6±0.0	n.d.	10.0±0.0	0.04±0.01	12.6±0.5	0.1±0.0	20.5±0.0	1.9±0.3	30.9±0.3
Se. yashadake	n.d.	5.2±0.0	n.d.	11.0±0.0	0.04±0.01	13.0±0.5	0.5±0.1	20.1±0.2	10.5±4.9	34.1±0.4
Se. fortis	n.d.	5.6±0.2	n.d.	11.0±0.0	0.05±0.002	12.8±0.6	1.0±0.1	22.4±1.1	7.0±2.5	31.9±0.3
Se. kagamiana	n.d.	5.2±0.0	n.d.	11.0±0.0	0.1±0.0	12.4±0.2	1.0±0.4	22.0±0.9	8.8±3.6	31.8±0.3
Pl. hindsii	n.d.	7.4±0.0	n.d.	11.7±0.0	0.1±0.0	16.8±0.9	0.1±0.0	22.1±0.1	0.2±0.2	29.7±1.2
Pl. linearis	n.d.	7.6±0.0	n.d.	11.3±0.0	0.2±0.1	13.9±0.6	0.1±0.1	20.7±0.4	1.8±1.5	27.6±1.7
Pl. simonii	n.d.	7.3±0.0	n.d.	10.6±0.0	0.1±0.1	12.0±0.6	0.1±0.0	19.5 ±1.6	0.1±0.1	24.4±0.3
Pl. chino	n.d.	4.8±0.0	n.d.	9.9±0.0	0.1±0.0	12.0±0.9	0.1±0.0	19.7±1.4	3.0±1.7	24.7±0.9
S. tsuboiana	n.d.	5.5±0.0	n.d.	9.9±0.0	n.d.	12.0±0.0	0.1±0.0	20.1±0.3	n.d.	24.4±0.3
S. veitchii	n.d.	7.2±0.0	n.d.	9.8±0.0	n.d.	12.5±0.0	0.1±0.0	23.6±0.2	n.d.	27.3±1.7
S. chartacea	n.d.	6.7±0.0	n.d.	10.0±0.0	n.d.	12.1±0.0	0.1±0.0	21.8±0.4	0.1±0.2	28.3±0.7
Sa. ramosa	n.d.	4.9±0.0	n.d.	9.8±0.0	n.d.	12.0±0.0	n.d.	23.2±0.2	n.d.	25.8±0.7
Sa. hortensis	n.d.	4.9±0.0	n.d.	9.8±0.0	n.d.	12.0±0.0	n.d.	23.2±0.0	n.d.	25.8±0.0

n.d.: No detection.

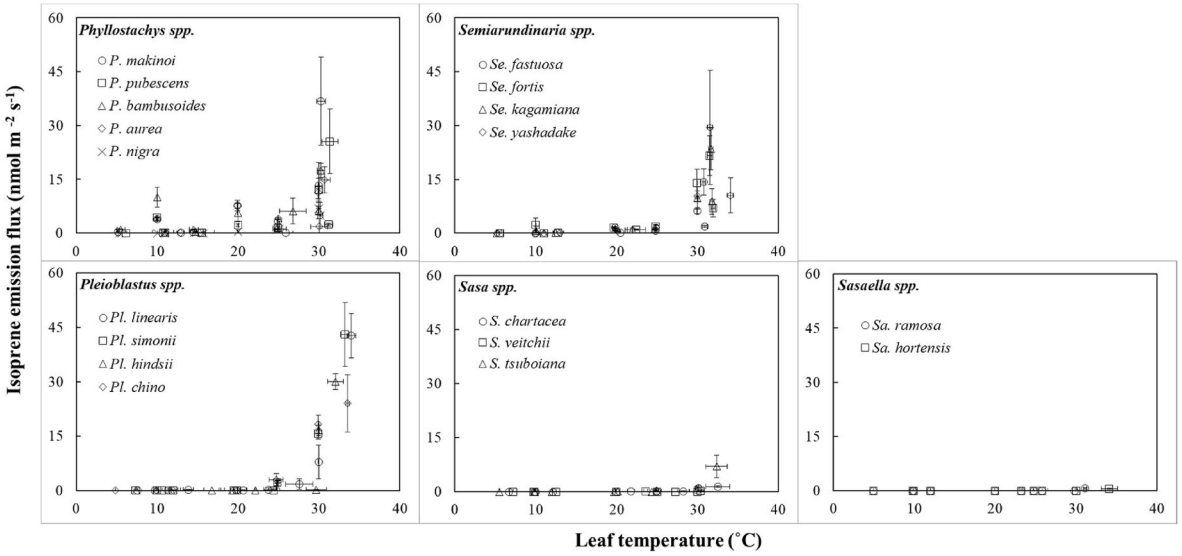

Fig. 2. Isoprene emission flux in response to leaf temperature for 18 species of bamboo within five genera from August 2019 to May 2020. The open circles are averaged observations of each species in each month (three measurements). The vertical and horizontal error bars represent standard deviation of isoprene emission flux and leaf temperature, respectively.

form demonstrated a correlation with LMA, a spurious correlation might exist between them. To exclude the effect of the potential spurious correlation, the isoprene emission flux against ETR in mass-based units was also tested. The results show that I_{Mass} increased with ETR_{Mass} in August and September 2019 for the tall species but was less definitive compared to those in area-base units and no correlation was seen when the observations during August and September 2019 for the tall species were included (Fig. 5).

The tall species exhibited extremely positive correlations between I_{Area} and A_{Area} in August and September 2019 (Table 3a); no correlation was exhibited by the dwarf species (Table 3b). Part of the correlation between I_{Area} and ETR_{Area} might be due to the spurious correlation from the LMA. I_{Mass} also increased with A_{Mass} in August and September 2019 for the tall species (Fig. 6), but with a lower correlation compared to I_{Area} and A_{Area} (Table 3a).

The photosynthetic rate did not show a large difference between the tall species and dwarf species. Due to the difference in isoprene emission, the ratio of carbon emitted as isoprene to carbon fixed by net photosynthetic (Carbon ratio (%) = I_{Area} (μmol m^{-2} s^{-1}) ÷ A_{Area} (μmol m^{-2} s^{-1})) indicated a large variation. Tall species in August and September 2019 exhibited average carbon ratios of 1.6 % and 0.6 %, respectively; carbon ratios observed in the dwarf species in August and September 2019 were much lower, at approximately 0.1 % and 0.0 %, respectively (Table 4).

4. Discussion

The results obtained from isoprene emission measurements of bamboo from August 2019 to May 2020 indicate clear differences in isoprene emission flux from the bamboo species under higher temperatures; all the species exhibited very low or no isoprene emissions during the measurement from October 2019 to April 2020. The isoprene

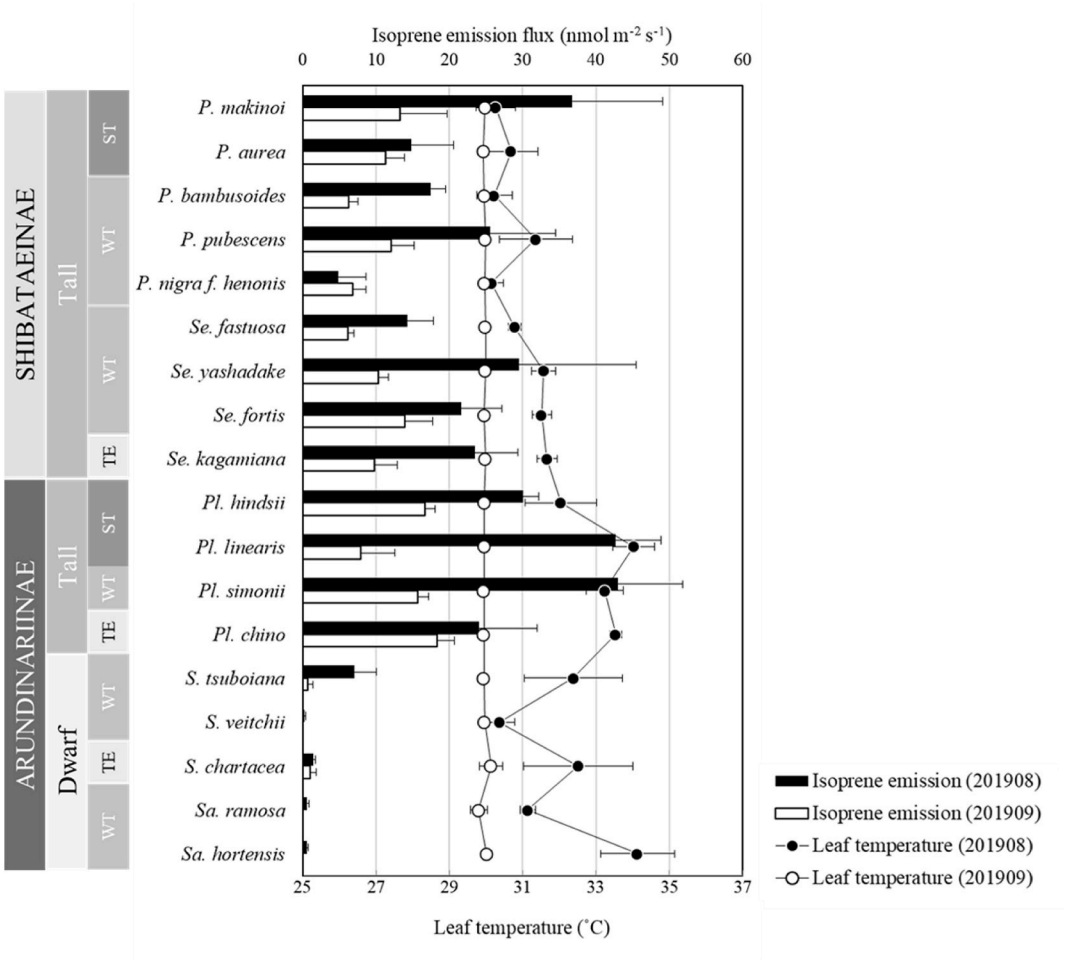

Fig. 3. Isoprene emission flux and leaf temperature of 18 bamboo species observed in August and September 2019. Solid bars and open bars represent mean isoprene emission flux with error bars representing standard deviation during August and September 2019, respectively; Solid circles and open circles represent mean leaf temperature with error bars representing standard deviation during August and September 2019, respectively. TE, WT, and ST are the climate of the region of origin of the species, which stand for temperate, warm temperate, and subtropical, respectively. *Arundinariinae* and *Shibataeinae* are subtribes under *Arundinarieae* tribe. Tall and dwarf represent two different growth types in bamboo stem.

emissions from certain species indicated a threshold-like dependence on leaf temperature, where larger fluxes were observed when the leaf temperature was >25 °C. Under the condition of lower leaf temperature, all the species exhibited very low or no emission of isoprene, and thus no significant difference was observed between isoprene emission rates among the species. This temperature dependency on seasonality could be explained by long-term control of the genetic expression of IspS with temperature (Oku et al., 2014; Mutanda et al., 2016). A similar phenomenon was previously reported by Chang et al. (2019), whereby isoprene emission measurements of *P. pubescens* in Taiwan demonstrated a temperature threshold of approximately 23 °C. Although the temperature gradually increased from February 2020 and reached to a temperature higher than the threshold in May 2020, low isoprene emissions even from high emitter species were observed from the bamboos. This might be due to the aging of the leaves for most of the species or the low isoprene emission capacity of newly expanded leaves for a certain species (i.e., *Pl. chino*), as indicated in previous studies (Niinemets et al., 2015; Funk et al., 1999).

To focus on the definitive variation in isoprene emission flux that occurs in the warmer season and to exclude the temperature dependence and other possible fluctuations in leaf phenology, we focused on the data measured in August and September 2019. We first hypothesized that the isoprene emission trait from bamboo species could be distinct either by growth type or by the climate of the region of origin of each species. As a result, a major difference was observed between the isoprene emission fluxes of the two different growth types (i.e., tall and dwarf), where the isoprene emission flux of tall bamboos ranged from 4.9 to 43.0 nmol m^{-2} s^{-1} in area-based unit and 24.6–157.8 μg g^{-1} h^{-1} in mass-based unit, while that of dwarf bamboos ranged from 0.2 to 7.0 nmol m^{-2} s^{-1} and 0.7–22.3 μg g^{-1} h^{-1}, respectively, in August. Okumura et al. (2018) recorded isoprene emission fluxes of 0.7–99.1 nmol m^{-2} s^{-1} of 14 bamboo species (*Phyllostachys* spp., *Tetragonocalamus* sp., *Sinobambusa* sp., *Bambusa* spp., *Semiarundinaria* spp., *Pseudosasa* sp., P*leioblastus* sp., and *Sasa* spp.). The high emitter genera reported by Okumura et al. (2018) were generally consistent with our result, however, a dwarf species (*Sasa kurilensis*) was observed with considerable emission (24.0 nmol m^{-2} s^{-1}). Comparing to this study, Okumura et al. (2018) demonstrated generally higher isoprene emission fluxes of *Phyllostachys* spp. (6.8–68.6 nmol m^{-2} s^{-1}) and *Semiarundinaria* spp. (53.6–57.8 nmol m^{-2} s^{-1}) under similar temperature of this study. The emission from tall bamboos is equivalent to the highest isoprene emissions under light intensity of 1000 μmol m^{-2} s^{-1} and leaf temperature of 30 °C have been recorded in *Populus* sp. (59 nmol m^{-2} s^{-1}; 165 μg g^{-1} h^{-1}), *Quercus* spp. (79 nmol m^{-2} s^{-1}; 157 μg g^{-1} h^{-1}), and *Salix* spp. (37 nmol m^{-2} s^{-1}; 133 μg g^{-1} h^{-1}) (Litvak et al., 1996; Geron et al., 2001; Chang et al., 2012). However, there is no evidence that isoprene emission rates differ among the origin climates. Species in the same genus tend to exhibit similar isoprene emission rates despite the fact that they might have different

Table 2
One-way ANOVA of the effect from climatic origins on isoprene emission fluxes for the tall and dwarf species in August and September 2019. A p-value ≤ 0.05 is needed to discard the null hypothesis that no significant difference in isoprene emission flux among the climatic origins.

	Sum of squared error	Degree of freedom	Mean squared error	F-ratio	p-value
Tall, August 2019					
Between Climates	601.64	2	300.82	1.96	0.16
Within Climates	5539.17	36	153.87		
Total	6140.81	38			
Tall, September 2019					
Between Climates	89.29	2	44.65	2.19	0.13
Within Climates	714.30	35	20.41		
Total	803.59	37			
Dwarf, August 2019					
Between Climates	1.08	1	1.08	0.12	0.73
Within Climates	116.14	13	8.93		
Total	117.22	14			
Dwarf, September 2019					
Between Climates	1.62	1	1.62	0.18	0.68
Within Climates	3.71	13	0.29		
Total	5.33	14			

origin climates.

A previous study indicated that the area-based isoprene emission flux could vary with LMA (Harley et al., 1997). Indeed, our results indicated a positive correlation between area-based isoprene emission flux and LMA across the tall species. Variation in LMA is usually related to acclimation to light environments, in which the leaves exposed to sunlight tend to exhibit higher LMA (Poorter et al., 2009). However, the light environments of all the species were unshaded and shared similar light profiles, regardless of growth types. Furthermore, the actual observation of LMA in August and September 2019 for the bamboo species exhibited no significant difference between the tall species and dwarf species. Therefore, we can exclude the possibility that the difference in isoprene emission flux between the two growth types was caused by variations in LMA. Indeed, higher isoprene fluxes were observed in the bamboo species with higher LMA, as the leaf thickness, and thus the concentration of chloroplasts where isoprene is produced, could affect the isoprene emission rate; nevertheless, it is only valid in the tall species.

Although major dependencies were recorded in leaf temperature and LMA, variation among leaves was still large. Previous studies have indicated the critical role of energetic and reducing agents in isoprene emission; the correlation between ETR and isoprene emission from multiple plant species (e.g., *Quercus* spp., *Eucalyptus* spp., and *Vismia guianensis*) has also been reported in several studies (Niinemets and Reichstein, 2002; Rapparini et al., 2004; Dani et al., 2015; Rodrigues et al., 2020). Furthermore, according to Farquhar et al. (1980), the photosynthetic rate is regulated by both intercellular CO_2 concentration, which is correlated to stomatal conductance, and electron transport. While the emission of isoprene is not limited to stomatal conductance (Sharkey, 1996), a much greater increase in isoprene emission flux could be expected under extremely high temperatures because photosynthesis reaches a maximum at lower temperatures (Niinemets et al., 1999; Rodrigues et al., 2020). Our results demonstrated definitive correlations among isoprene emission, photosynthetic rate, and ETR, which is consistent with previous results; even more definitive correlation was found with ETR_{Mass} than that with A_{Mass}. The relationship between isoprene emission flux and ETR could explain part of the discrepancy in isoprene emission flux across the tall species. This evidence suggests a dependence of isoprene emission on ETR. However, this is only adequate for the tall species. Moreover, despite a low total isoprene emission, the photosynthetic traits of the dwarf species were not significantly different from those of the tall species.

August and September 2019 showed obviously different isoprene emission traits to each other for the tall species, where September 2019 generally showed much lower isoprene emission rates and carbon ratios. One of the reasons of this change might be attributed to the response to T_L. Larger isoprene emission fluxes were found in August with higher leaf temperature, especially for *Pleioblastus* spp., which were consistent with the temperature dependence curve in Fig. 2. However, other reasons should be counted because some of the genera (i.e., *Phyllostachys* spp. and *Semiarundinaria* spp.) showed large decrease in isoprene emissions even under similar T_L between the two months. This might be partially attributed to the influence of ETR, where several species (e.g., *P. makinoi*, *P. bambusoides*, *P. pubescens*, *Se. fastuosa*, *Se. fortis*, *Se. kagamiana* and *Pl. linearis*) also showed a large decrease in ETR September (Table 4a). The other probability is the previous exposure of higher ambient temperature in August, as we attempted to manipulate T_L into 30 °C, lower T_L were recorded than that in ambient. Previous studies also indicated that leaf in different growth stage demonstrates different capacity of isoprene emission rate (Kuzma and Fall 1993; Monson et al., 1994). Thus, leaf phenological change could also influence the isoprene emission rate from August to September. According to meteorological data in Kyoto City, both August and September 2019 had remarkable monthly precipitation though August had much more precipitation than September 2019 (August: 355.0 mm; September: 84.5

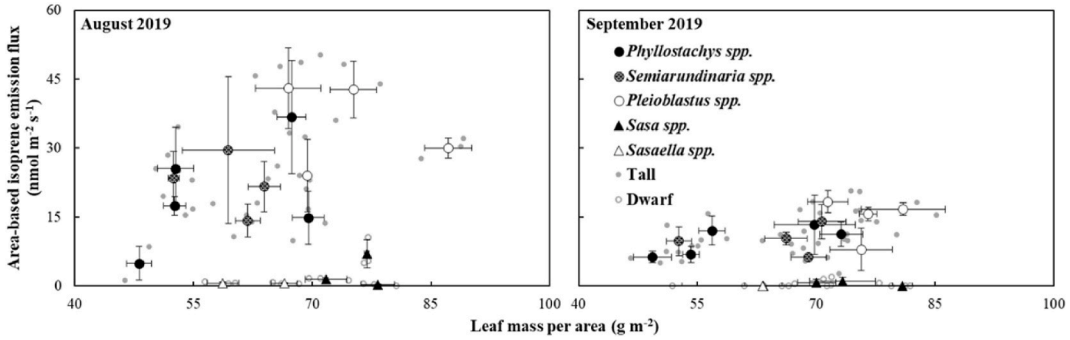

Fig. 4. Area-based isoprene emission flux in response to leaf mass per area for 18 species of bamboo within five genera observed in August and September 2019. Solid circles, dot-pattern circles, and diagonal-pattern circles, with error bars representing standard deviations, indicate averaged observations of each species in *Phyllostachys*, *Semiarundinaria,* and *Pleioblastus*, respectively; open triangles and dot-pattern triangles, with error bars representing standard deviations, indicate averaged observations of each species in *Sasa* and *Sasaella*, respectively. Solid gray dots and open gray dots represent observations in the tall species (*Phyllostachys*, *Semiarundinaria,* and *Pleioblastus* spp.) and the dwarf species (*Sasa* and *Sasaella* spp.), respectively.

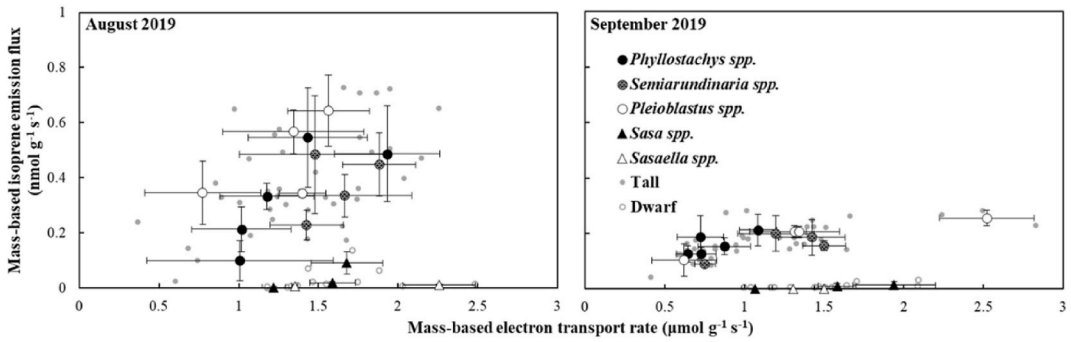

Fig. 5. Mass-based isoprene emission flux in response to mass-based electron transport rate for 18 species of bamboo within five genera observed in August and September 2019. Solid circles, dot-pattern circles, and diagonal-pattern circles, with error bars representing standard deviations, indicate averaged observations of each species in *Phyllostachys*, *Semiarundinaria,* and *Pleioblastus*, respectively; open triangles and dot-pattern triangles, with error bars representing standard deviations, indicate averaged observations of each species in *Sasa* and *Sasaella*, respectively. Solid gray dots and open gray dots represent observations in the tall species (*Phyllostachys*, *Semiarundinaria,* and *Pleioblastus* spp.) and the dwarf species (*Sasa* and *Sasaella* spp.), respectively.

Table 3a
Coefficient of determination (R^2) and p-value of each pair between area-based isoprene emission flux (I_{Area}), mass-based isoprene emission flux (I_{Mass}), leaf mass per area (*LMA*), area-based electron transport rate (ETR_{Area}), mass-based electron transport rate (ETR_{Mass}), area-based photosynthetic rate (A_{Area}), and mass-based photosynthetic rate (A_{Mass}) for 13 species of tall bamboos.

Aug 2019, Tall species	I_{Mass}		*LMA*		ETR_{Area}		ETR_{Mass}		A_{Area}		A_{Mass}	
	R^2	p-value	R^2	p-value	R^2	p-value	R^2	p-value	R^2	p-value	R^2	p-value
I_{Area}	0.896	***	0.237	**	0.378	***	0.168	**	0.257	***	0.099	
I_{Mass}			0.043		0.338	***	0.287	***	0.233	**	0.165	*
LMA					0.157	*	0.011		0.057		0.018	
ETR_{Area}							0.741	***	0.406	***	0.285	***
ETR_{Mass}									0.315	***	0.436	***
A_{Area}											0.843	***
Sep 2019, Tall species												
I_{Area}	0.853	***	0.277	***	0.542	***	0.418	***	0.472	***	0.355	***
I_{Mass}			0.032		0.434	***	0.448	***	0.242	**	0.277	***
LMA					0.177	**	0.030		0.463	***	0.137	*
ETR_{Area}							0.926	***	0.428	***	0.369	***
ETR_{Mass}									0.259	***	0.302	***
A_{Area}											0.856	***

*: statistically significant correlation (p-value ≤ 0.05) **: strong correlation (p-value ≤ 0.01) ***: very strong correlation (p-value ≤ 0.001)

mm). Also, based on our gas exchange results in A_{Area}, there were no clear evidence of drought stress both in August and September 2019 (Table 4a; 4b). Different from these species, *P. nigra* f. *henonis* did not showed large decrease in I_{Area}. Instead, it slightly increased in September under merely no change in T_L from August. Since *P. nigra* f. *henonis* later underwent a synchronous flowering which might largely disturb the physiology of the plant, the isoprene emission characteristics might be altered. Further investigation is needed to clarify the relationship between seasonal pattern of isoprene emission flux of bamboo species and synchronous flowering event. Since the effects of previous exposure to ambient temperature and leaf phenology on isoprene emission were not directly observed in this study, further investigation is suggested for bamboo species.

Typically, carbon loss from isoprene emission in assimilation usually accounts for approximately 1–2 % at 30 °C and depends on the photosynthetic rate; under extremely high temperatures, the isoprene emission could account for more than 50 % of carbon loss (Tingey et al., 1979; Harley et al., 1994; Tani and Kawawata, 2008; Morfopoulos et al., 2014). Okumura et al. (2018) reported a range of 0–1.5 % of carbon loss from isoprene emissions in multiple bamboo species during summer. This study observed that the average carbon ratio for tall bamboo species was 1.6 % and 0.6 % in August and September 2019, respectively; certain species can reach a carbon ratio of 2.7 % during *a* T_L of 32 °C. In contrast, the dwarf bamboo species used very low carbon for isoprene

Table 3b
Coefficient of determination (R^2) and p-value of each pair between area-based isoprene emission flux (I_{Area}), mass-based isoprene emission flux (I_{Mass}), leaf mass per area (*LMA*), area-based electron transport rate (ETR_{Area}), mass-based electron transport rate (ETR_{Mass}), area-based photosynthetic rate (A_{Area}), and mass-based photosynthetic rate (A_{Mass}) for 5 species of dwarf bamboos.

	I_{Mass}		*LMA*		ETR_{Area}		ETR_{Mass}		A_{Area}		A_{Mass}	
Aug 2019, Dwarf species	R^2	p-value	R^2	p-value	R^2	p-value	R^2	p-value	R^2	p-value	R^2	p-value
I_{Area}	0.999	***	0.145		0.207		0.012		0.028		0.069	
I_{Mass}			0.128		0.222		0.018		0.027		0.063	
LMA					0.058		0.466	**	0.028		0.049	
ETR_{Area}							0.749	***	0.123		0.234	
ETR_{Mass}									0.054		0.282	*
A_{Area}											0.839	***
Sep 2019, Dwarf species												
I_{Area}	0.999	**	0.014		0.544	**	0.486	**	0.047		0.037	
I_{Mass}			0.013		0.538	**	0.485	**	0.047		0.036	
LMA					0.073		0.023		0.108		0.022	
ETR_{Area}							0.827	***	0.447	**	0.404	*
ETR_{Mass}									0.324	*	0.379	*
A_{Area}											0.958	***

*: statistically significant correlation (p-value ≤ 0.05) **: strong correlation (p-value ≤ 0.01) ***: very strong correlation (p-value ≤ 0.001)

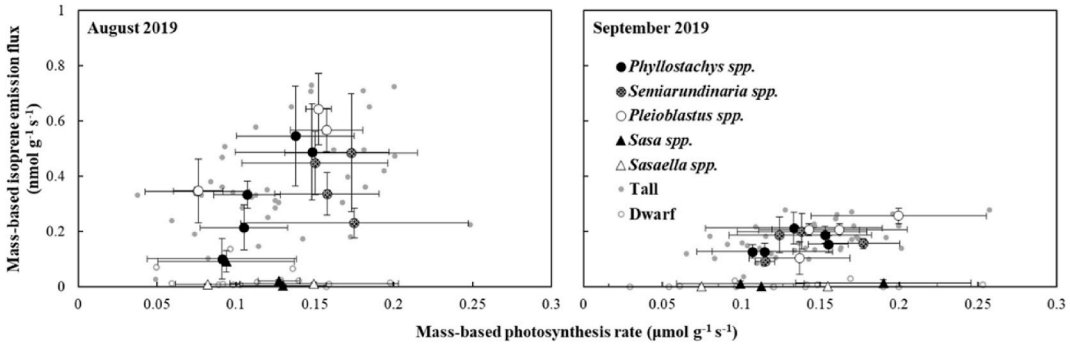

Fig. 6. Mass-based isoprene emission flux in response to mass-based photosynthetic rate for 18 species of bamboo within five genera observed in August and September 2019. Solid circles, dot-pattern circles, and diagonal-pattern circles, with error bars representing standard deviations, indicate averaged observations of each species in *Phyllostachys*, *Semiarundinaria,* and *Pleioblastus*, respectively; open triangles and dot-pattern triangles, with error bars representing standard deviations, indicate averaged observations of each species in *Sasa* and *Sasaella*, respectively. Solid gray dots and open gray dots represent each observation in the tall species (*Phyllostachys*, *Semiarundinaria,* and *Pleioblastus* spp.) and the dwarf species (*Sasa* and *Sasaella* spp.), respectively.

emissions, which was usually less than 0.2 %. This difference is very reasonable because dwarf bamboos usually grow in the understory of forest areas, where heat stress is less due to indirect sunlight. Moreover, to adapt to low light conditions, preventing loss of carbon could be a critical life strategy by dwarf bamboos. Nonetheless, in our study, the dwarf species was exposed to direct sunlight, which is unnatural. This implies that the low isoprene emission capacity is genetically determined in case of the dwarf species, as plants lacking the IspS gene are unable to produce isoprene (Behnke et al., 2007).

5. Conclusion

Based on observations in isoprene emission flux and related factors such as LMA, ETR, and photosynthetic rate of 18 bamboo species, the study suggests a distinction in isoprene emissions between the tall and dwarf bamboos, which is genetically determined. This difference in genotype causes different dependencies of isoprene emission on leaf temperature, LMA, photosynthetic rate, and ETR.

CRediT authorship contribution statement

Ting-Wei Chang: Conceptualization, Formal analysis, Investigation, Methodology, Data curation, Writing – original draft, Visualization. **Yoshiko Kosugi:** Writing – review & editing, Supervision, Resources, Project administration, Funding acquisition. **Motonori Okumura:** Methodology, Funding acquisition. **Linjie Jiao:** Investigation. **Siyu**

Table 4a
Area-based isoprene emission (I_{Area}), area-based photosynthetic rate (A_{Area}), carbon ration, leaf temperature (T_L), and area-based electron transport rate (ETR_{Area}) in August and September 2019 for 13 species of tall bamboos. The values are represented in mean ± standard deviation.

Genus	Species	I_{Area} (nmol m^{-2} s^{-1})		A_{Area} (μmol m^{-2} s^{-1})		Carbon ratio (%)		T_L (°C)		ETR_{Area} (μmol m^{-2} s^{-1})	
		Aug 2019	Sep 2019	Aug 2019	Sep 2019	Aug 2019	Sep 2019	Aug 2019	Sep 2019	Aug 2019	Sep 2019
Phyllostachys	*P. makinoi*	36.8±12.3	13.3±6.4	9.3±2.7	10.7±2.4	2.0±0.6	0.6±0.2	30.3±0.5	30.0±0.1	96.9±26.8	51.0±13.8
	P. aurea	14.9±5.7	11.3±2.6	7.3±1.8	11.3±1.0	1.0±0.4	0.5±0.1	30.7±0.7	29.9±0.0	70.9±22.5	63.9±12.3
	P. bambusoides	17.5±2.1	6.3±1.2	5.7±1.2	5.2±1.0	1.6±0.6	0.6±0.1	30.2±0.5	30.0±0.0	62.2±17.1	35.9±5.2
	P. pubescens	25.6±8.9	12.1±3.2	7.9±2.8	7.6±3.4	1.8±0.9	0.9±0.4	31.4±1.0	30.0±0.0	101.7±16.4	61.6±5.4
	P. nigra f. henonis	4.9±3.7	6.9±1.7	4.4±2.4	6.2±2.3	0.5±0.2	0.6±0.3	30.2±0.3	30.0±0.0	49.0±29.6	34.9±3.3
	Average	19.9±12.8	10.0±4.2	6.9±2.6	8.2±3.1	1.4±0.7	0.6±0.2	30.5±0.7	30.0±0.0	76.1±28.6	49.5±14.8
Semiarundinaria	*Se. fastuosa*	14.2±3.6	6.2±0.8	10.8±4.5	7.9±0.2	0.8±0.5	0.4±0.0	30.8±0.2	30.0±0.0	88.2±13.9	51.9±3.0
	Se. yashadake	29.5±15.9	10.3±1.4	10.3±3.0	11.8±1.8	1.4±0.4	0.4±0.1	31.6±0.3	30.0±0.0	89.1±36.1	99.4±11.5
	Se. fortis	21.6±5.5	14.0±3.7	10.1±2.4	9.7±2.6	1.1±0.1	0.8±0.1	31.5±0.3	29.9±0.0	107.1±29.9	84.2±13.5
	Se. kagamiana	23.5±5.8	9.8±3.1	7.9±2.5	6.5±1.5	1.5±0.4	0.7±0.1	31.7±0.3	30.0±0.0	98.8±13.1	74.8±9.2
	Average	22.2±9.6	9.7±3.4	9.8±3.0	9.0±2.5	1.2±0.4	0.6±0.2	31.4±0.4	30.0±0.0	95.8±23.1	77.6±20.0
Pleioblastus	*Pl. hindsii*	30.0±2.2	16.7±1.4	6.6±3.0	13.1±3.4	2.7±1.5	0.7±0.1	32.0±1.0	30.0±0.1	121.8±9.1	105.7±18.5
	Pl. linearis	42.7±6.1	7.9±4.6	11.8±1.7	10.4±2.9	1.9±0.5	0.4±0.2	34.0±0.6	30.0±0.0	100.7±31.2	47.6±17.8
	Pl. simonii	43.0±8.8	15.7±1.4	10.2±0.8	10.9±2.5	2.1±0.5	0.8±0.2	33.2±0.5	29.9±0.0	104.9±19.7	102.8±2.1
	Pl. chino	24.0±7.9	18.3±2.4	5.3±1.1	14.4±4.5	2.2±0.3	0.7±0.1	33.5±0.2	29.9±0.0	53.7±25.2	180.3±22.3
	Average	34.9±10.3	14.6±4.8	8.5±3.2	12.2±3.3	2.2±0.8	0.6±0.2	33.2±0.9	29.9±0.0	95.3±32.8	109.1±51.4
Average		25.2±12.7	11.4±4.7	8.3±3.1	9.7±3.4	1.6±0.8	0.6±0.2	31.6±1.3	30.0±0.0	88.1±29.3	76.5±39.8

Table 4b
Area-based isoprene emission (I_{Area}), area-based photosynthetic rate (A_{Area}), carbon ration, leaf temperature (T_L), and area-based electron transport rate (ETR_{Area}) in August and September 2019 for 5 species of dwarf bamboos. The values are represented in mean ± standard deviation.

Genus	Species	I_{Area} (nmol m^{-2} s^{-1})		A_{Area} (μmol m^{-2} s^{-1})		Carbon ratio (%)		T_L (°C)		ETR_{Area} (μmol m^{-2} s^{-1})	
		Aug 2019	Sep 2019	Aug 2019	Sep 2019	Aug 2019	Sep 2019	Aug 2019	Sep 2019	Aug 2019	Sep 2019
Sasa	*S. tsuboiana*	7.0±3.1	0.7±0.7	7.2±3.3	6.9±2.6	0.6± 0.3	0.1±0.1	32.4±1.3	29.9±0.0	129.1±16.9	110.8±8.8
	S. veitchii	0.2±0.2	n.d.	10.2±2.4	9.1±1.0	0.0±0.0	0.0±0.0	30.4±0.4	30.0±0.0	95.5±5.8	86.3±5.6
	S. chartacea	1.4±0.2	1.0±0.9	9.1±0.7	13.8±3.4	0.1±0.0	0.0±0.0	32.5±1.5	30.1±0.3	113.9±11.1	141.5±12.0
	Average	2.9±3.5	0.6±0.7	8.8±2.5	9.9±3.8	0.2±0.3	0.0±0.0	31.8±1.5	30.0±0.2	112.8±18.0	112.9±25.3
Sasaella	*Sa. Ramosa*	0.6±0.2	n.d.	8.7±2.9	9.8±4.4	0.0±0.0	0.0±0.0	31.1±0.2	29.8±0.2	132.3±9.1	94.9±6.0
	Sa. Hortensis	0.5±0.2	n.d.	5.5±1.5	5.1±4.4	0.1±0.0	0.0±0.0	34.1±1.0	30.0±0.1	89.9±0.9	83.6±20.9
	Average	0.6±0.2	n.d.	7.1±2.7	7.4±4.7	0.0±0.0	0.0±0.0	32.6±1.8	29.9±0.2	111.1±23.9	89.2±15.1
Average		2.0±2.9	0.3±0.6	8.1±2.6	8.9±4.2	0.1±0.2	0.0±0.0	32.1±1.6	30.0±0.2	112.1±19.7	103.4±24.3

Chen: Investigation. **Dingkang Xu:** Investigation. **Zhining Liu:** Investigation. **Shozo Shibata:** Resources. **Ken-Hui Chang:** Methodology, Resources.

Declaration of competing interest

The authors declare that they have no known competing financial interests or personal relationships that could have appeared to influence the work reported in this paper.

Acknowledgement

This work was supported by The Coca-Cola Foundation and JSPS KAKENHI [grant number 21K12275]. We would like to express appreciation to Field Science Education and Research Center of Kyoto University (FSERC) for providing site and bamboo material. We would also like to express appreciation to Dr. Yeou-Lih Yan (Professor of Department of Safety, Health and Environmental Engineering, National United University), and Mrs. Yi-Jen Pan (Research Assistant of Department of Safety, Health and Environmental Engineering, National Yunlin University of Science and Technology) to provide technical supports in VOCs analysis.

References

Archibald, A.T., Levine, J.G., Abraham, N.L., Cooke, M.C., Edwards, P.M., Heard, D.E., Jenkin, M.E., Karunaharan, A., Pike, R.C., Monks, P.S., Shallcross, D.E., Telford, P.J., Whalley, L.K., Pyle, J.A., 2011. Impacts of HO_x regeneration and recycling in the oxidation of isoprene: consequences for the composition of past, present and future atmospheres. Geophys. Res. Lett. 38 (5), L05804. https://doi.org/10.1029/2010GL046520.

Behnke, K., Ehlting, B., Teuber, M., Bauerfeind, M., Louis, S., Hänsch, R., Polle, A., Bohlmann, J., Schnitzler, J.P., 2007. Transgenic, non-isoprene emitting poplars don't like it hot. Plant J. 51 (3), 485–499. https://doi.org/10.1111/j.1365-313x.2007.03157.x.

Biesenthal, T.A., Wu, Q., Shepson, P.B., Wiebe, H.A., Anlauf, K.G., Mackay, G.I., 1997. A study of relationships between isoprene, its oxidation products, and ozone, in the Lower Fraser Valley, BC. Atmos. Environ. 31 (14), 2049–2058. https://doi.org/10.1016/S1352-2310(96)00318-4.

Brüggemann, N., Schnitzler, J.-P., 2002. Diurnal variation of dimethylallyl diphosphate concentrations in oak (*Quercus robur*) leaves. Physiol. Plantarum 115 (2), 190–196. https://doi.org/10.1034/j.1399-3054.2002.1150203.x.

Chang, J., Ren, Y., Shi, Y., Zhu, Y., Ge, Y., Hong, S., Jiao, L., Lin, F., Peng, C., Mochizuki, T., Tani, A., Mu, Y., Fu, C., 2012. An inventory of biogenic volatile organic compounds for a subtropical urban–rural complex. Atmos. Environ. 56, 115–123. https://doi.org/10.1016/j.atmosenv.2012.03.053.

Chang, T., Kume, T., Okumura, M., Kosugi, Y., 2019. Characteristics of isoprene emission from moso bamboo leaves in a forest in central Taiwan. Atmos. Environ. 211, 288–295. https://doi.org/10.1016/j.atmosenv.2019.05.026.

Claeys, M., Graham, B., Vas, G., Wang, W., Vermeylen, R., Pashynska, V., Cafmeyer, J., Guyon, P., Andreae, M.O., Artaxo, P., Maenhaut, W., 2004a. formation of secondary organic aerosols through photooxidation of isoprene. Science 303 (5661), 1173–1176. https://doi.org/10.1126/science.1092805.

Claeys, M., Wang, W., Ion, A.C., Kourtchev, I., Gelencsér, A., Maenhaut, W., 2004b. Formation of secondary organic aerosols from isoprene and its gas-phase oxidation products through reaction with hydrogen peroxide. Atmos. Environ. 38 (25), 4093–4098. https://doi.org/10.1016/j.atmosenv.2004.06.001.

Clark, L.G., Londoño, X., Ruiz-Sanchez, E., 2015. Bamboo taxonomy and habitat. In: Liese, Walter, Köhl, Michael (Eds.), Bamboo: the Plant and its Uses (1-30). Springer International Publishing. https://doi.org/10.1007/978-3-319-14133-6_1.

Collins, W.J., Derwent, R.G., Johnson, C.E., Stevenson, D.S., 2002. The oxidation of organic compounds in the troposphere and their global warming potentials. Climatic Change 52 (4), 453–479. https://doi.org/10.1023/A:1014221225434.

Dani, K.G.S., Jamie, I.M., Prentice, I.C., Atwell, B.J., 2015. Species-specific photorespiratory rate, drought tolerance and isoprene emission rate in plants. Plant Signal. Behav. 10 (3), e990830 https://doi.org/10.4161/15592324.2014.990830.

Dreyfus, G.B., Schade, G.W., Goldstein, A.H., 2002. Observational constraints on the contribution of isoprene oxidation to ozone production on the western slope of the Sierra Nevada, California. J. Geophys. Res. 107 (D19), 4365. https://doi.org/10.1029/2001JD001490.

Duane, M., Poma, B., Rembges, D., Astorga, C., Larsen, B.R., 2002. Isoprene and its degradation products as strong ozone precursors in Insubria, Northern Italy. Atmos. Environ. 36 (24), 3867–3879. https://doi.org/10.1016/S1352-2310(02)00359-X.

Farquhar, G.D., von Caemmerer, S., Berry, J.A., 1980. A biochemical model of photosynthetic CO_2 assimilation in leaves of C_3 species. Planta 149 (1), 78–90. https://doi.org/10.1007/BF00386231.

Fierravanti, A., Fierravanti, E., Cocozza, C., Tognetti, R., Rossi, S., 2017. Eligible reference cities in relation to BVOC-derived O_3 pollution. Urban For. Urban Green. 28, 73–80. https://doi.org/10.1016/j.ufug.2017.09.012.

Funk, J.L., Jones, C.G., Lerdau, M.T., 1999. Defoliation effects on isoprene emission from *Populus deltoides*. Oecologia 118 (3), 333–339. https://doi.org/10.1007/s004420050734.

Geng, F., Tie, X., Guenther, A., Li, G., Cao, J., Harley, P., 2011. Effect of isoprene emissions from major forests on ozone formation in the city of Shanghai, China. Atmos. Chem. Phys. 11 (20), 10449–10459. https://doi.org/10.5194/acp-11-10449-2011.

Geron, C., Harley, P., Guenther, A., 2001. Isoprene emission capacity for US tree species. Atmos. Environ. 35 (19), 3341–3352. https://doi.org/10.1016/S1352-2310(00)00407-6.

Guenther, A., Karl, T., Harley, P., Wiedinmyer, C., Palmer, P.I., Geron, C., 2006. Estimates of global terrestrial isoprene emissions using MEGAN (model of emissions of gases and aerosols from nature). Atmos. Chem. Phys. 6 (11), 3181–3210. https://doi.org/10.5194/acp-6-3181-2006.

Guenther, A.B., Jiang, X., Heald Colette, L., Sakulyanontvittaya, T., Duhl, T., Emmons, L. K., Wang, X., 2012. The model of emissions of gases and aerosols from nature version 2.1 (MEGAN2.1): an extended and updated framework for modeling biogenic emissions. Geosci. Model Dev. (GMD) 5 (6), 1471–1492.

Harley, P.C., Litvak, M.E., Sharkey, T.D., Monson, R.K., 1994. Isoprene emission from velvet bean leaves (interactions among nitrogen availability, growth photon flux density, and leaf development). Plant Physiol. 105 (1), 279–285. https://doi.org/10.1104/pp.105.1.279.

Harley, P., Guenther, A., Zimmerman, P., 1997. Environmental controls over isoprene emission in deciduous oak canopies. Tree Physiol. 17 (11), 705–714. https://doi.org/10.1093/treephys/17.11.705.

Kamens, R.M., Gery, M.W., Jeffries, H.E., Jackson, M., Cole, E.I., 1982. Ozone–isoprene reactions: product formation and aerosol potential. Int. J. Chem. Kinet. 14, 955–975. https://doi.org/10.1002/kin.550140902.

Kanakidou, M., Seinfeld, J.H., Pandis, S.N., Barnes, I., Dentener, F.J., Facchini, M.C., Van Dingenen, R., Ervens, B., Nenes, A., Nielsen, C.J., Swietlicki, E., Putaud, J.P., Balkanski, Y., Fuzzi, S., Horth, J., Moortgat, G.K., Winterhalter, R., Myhre, C.E.L., Tsigaridis, K., Vignati, E., Stephanou, E.G., Wilson, J., 2005. Organic aerosol and global climate modelling: a review. Atmos. Chem. Phys. 5 (4), 1053–1123. https://doi.org/10.5194/acp-5-1053-2005.

Kleinhenz, V., Midmore, D.J., 2001. Aspects of bamboo agronomy. Adv. Agron. 74, 99–153. https://doi.org/10.1016/S0065-2113(01)74032-1.

Kroll, J.H., Ng, N.L., Murphy, S.M., Flagan, R.C., Seinfeld, J.H., 2005. Secondary organic aerosol formation from isoprene photooxidation under high-NO_x conditions. Geophys. Res. Lett. 32, L18808. https://doi.org/10.1029/2005GL023637.

Kroll, J.H., Ng, N.L., Murphy, S.M., Flagan, R.C., Seinfeld, J.H., 2006. Secondary organic aerosol formation from isoprenephotooxidation. Environ. Sci. Technol. 40, 1869–1877. https://doi.org/10.1021/es0524301.

Kudo, G., Amagai, Y., Hoshino, B., Kaneko, M., 2011. Invasion of dwarf bamboo into alpine snow-meadows in northern Japan: pattern of expansion and impact on species diversity. Ecology and Evolution 1, 85–96. https://doi.org/10.1002/ece3.9.

Kuzma, J., Fall, R., 1993. Leaf isoprene emission rate is dependent on leaf development and the level of isoprene synthase. Plant Physiol. 101 (2), 435–440. https://doi.org/10.1104/pp.101.2.435.

Li, R., During, H.J., Werger, M.J.A., Zhong, Z.C., 1998a. Positioning of new shoots relative to adult shoots in groves of giant bamboo, *Phyllostachys pubescens*. Flora 193 (3), 315–321. https://doi.org/10.1016/S0367-2530(17)30852-6.

Li, R., Werger, M.J.A., During, H.J., Zhong, Z.C., 1998b. Biennial variation in production of new shoots in groves of the giant bamboo *Phyllostachys pubescens* in Sichuan, China. Plant Ecol. 135 (1), 103–112. https://doi.org/10.1023/A:1009761428401.

Liakoura, V., Fotelli, M.N., Rennenberg, H., Karabourniotis, G., 2009. Should structure-function relations be considered separately for homobaric vs. heterobaric leaves? Am. J. Bot. 96, 612–619. https://doi.org/10.3732/ajb.0800166.

Lichtenthaler, H.K., 1999. The 1-deoxy-D-xylulose-5-phosphate pathway of isoprenoid biosynthesis in plants. Annu. Rev. Plant Physiol. Plant Mol. Biol. J50, 47–65. https://doi.org/10.1146/annurev.arplant.50.1.47.

Litvak, M.E., Loreto, F., Harley, P.C., Sharkey, T.D., Monson, R.K., 1996. The response of isoprene emission rate and photosynthetic rate to photon flux and nitrogen supply in aspen and white oak trees. Plant Cell Environ. 19 (5), 549–559. https://doi.org/10.1111/j.1365-3040.1996.tb00388.x.

Loreto, F., Velikova, V., 2001. Isoprene produced by leaves protects the photosynthetic apparatus against ozone damage, quenches ozone products, and reduces lipid peroxidation of cellular membranes. Plant Physiol. 127 (4), 1781–1787. https://doi.org/10.1104/pp.010497.

Monson, R.K., Harley, P.C., Litvak, M.E., Wildermuth, M., Guenther, A.B., Zimmerman, P.R., Fall, R., 1994. Environmental and developmental controls over the seasonal pattern of isoprene emission from aspen leaves. Oecologia 99 (3), 260–270. https://doi.org/10.1007/BF00627738.

Monson, R.K., Grote, R., Niinemets, Ü., Schnitzler, J.-P., 2012. Modeling the isoprene emission rate from leaves. New Phytol. 195 (3), 541–559. https://doi.org/10.1111/j.1469-8137.2012.04204.x.

Monson, R.K., Jones, R.T., Rosenstiel, T.N., Schnitzler, J.-P., 2013. Why only some plants emit isoprene. Plant Cell Environ. 36, 503–516. https://doi.org/10.1111/pce.12015.

Morfopoulos, C., Sperlich, D., Peñuelas, J., Filella, I., Llusià, J., Medlyn, B.E., Niinemets, Ü., Possell, M., Sun, Z., Prentice, I.C., 2014. A model of plant isoprene emission based on available reducing power captures responses to atmospheric CO_2. New Phytol. 203 (1), 125–139. https://doi.org/10.1111/nph.12770.

Mutanda, I., Saitoh, S., Inafuku, M., Aoyama, H., Takamine, T., Satou, K., Akutsu, M., Teruya, K., Tamotsu, H., Shimoji, M., Sunagawa, H., Oku, H., 2016. Gene expression analysis of disabled and re-induced isoprene emission by the tropical tree *Ficus septica* before and after cold ambient temperature exposure. Tree Physiol. 36 (7), 873–882. https://doi.org/10.1093/treephys/tpw032.

Niinemets, Ü., Tenhunen, J.D., Harley, P.C., Steinbrecher, R., 1999. A model of isoprene emission based on energetic requirements for isoprene synthesis and leaf photosynthetic properties for *Liquidambar* and *Quercus*. Plant Cell Environ. 22 (11), 1319–1335. https://doi.org/10.1046/j.1365-3040.1999.00505.x.

Niinemets, Ü., Reichstein, M., 2002. A model analysis of the effects of nonspecific monoterpenoid storage in leaf tissues on emission kinetics and composition in Mediterranean sclerophyllous *Quercus* species. Global Biogeochem. Cycles 16 (4), 1110. https://doi.org/10.1029/2002GB001927.

Niinemets, Ü., Keenan, T.F., Hallik, L., 2015. A worldwide analysis of within-canopy variations in leaf structural, chemical and physiological traits across plant functional types. New Phytol. 205 (3), 973–993. https://doi.org/10.1111/nph.13096.

Oku, H., Inafuku, M., Takamine, T., Nagamine, M., Saitoh, S., Fukuta, M., 2014. Temperature threshold of isoprene emission from tropical trees, *Ficus virgata* and *Ficus septica*. Chemosphere 95, 268–273. https://doi.org/10.1016/j.chemosphere.2013.09.003.

Okumura, M., Kosugi, Y., Tani, A., 2018. Biogenic volatile organic compound emissions from bamboo species in Japan. J. Agric. Meteorol. 74 (1), 40–44. https://doi.org/10.2480/agrmet.D-17-00017.

Okutomi, K., Shinoda, S., Fukuda, H., 1996. Causal analysis of the invasion of broad-leaved forest by bamboo in Japan. J. Veg. Sci. 7 (5), 723–728. https://doi.org/10.2307/3236383.

Pang, X., Mu, Y., Zhang, Y., Lee, X., Yuan, J., 2009. Contribution of isoprene to formaldehyde and ozone formation based on its oxidation products measurement in Beijing, China. Atmos. Environ. 43 (13), 2142–2147. https://doi.org/10.1016/j.atmosenv.2009.01.022.

Paulson, S.E., Flagan, R.C., Seinfeld, J.H., 1992. Atmospheric photooxidation of isoprene part I: the hydroxyl radical and ground state atomic oxygen reactions. Int. J. Chem. Kinet. 24, 79–101. https://doi.org/10.1002/kin.550240109.

Paulson, S.E., Seinfeld, J.H., 1992. Development and evaluation of a photooxidation mechanism for isoprene. J. Geophys. Res. 97 (D18), 20703–20715. https://doi.org/10.1029/92JD01914.

Pike, R.C., Young, P.J., 2009. How plants can influence tropospheric chemistry: the role of isoprene emissions from the biosphere. Weather 64 (12), 332–336. https://doi.org/10.1002/wea.416.

Poisson, N., Kanakidou, M., Crutzen, P.J., 2000. Impact of non-methane hydrocarbons on tropospheric chemistry and the oxidizing power of the global troposphere: 3-dimensional modelling results. J. Atmos. Chem. 36 (2), 157–230. https://doi.org/10.1023/A:1006300616544.

Poorter, H., Niinemets, Ü., Poorter, L., Wright, I.J., Villar, R., 2009. Causes and consequences of variation in leaf mass per area (LMA): a meta-analysis. New Phytol. 182 (3), 565–588. https://doi.org/10.1111/j.1469-8137.2009.02830.x.

Rapparini, F., Baraldi, R., Miglietta, F., Loreto, F., 2004. Isoprenoid emission in trees of *Quercus pubescens* and *Quercus ilex* with lifetime exposure to naturally high CO_2 environment. Plant Cell Environ. 27 (4), 381–391. https://doi.org/10.1111/j.1365-3040.2003.01151.x.

Rasulov, B., Hüve, K., Välbe, M., Laisk, A., Niinemets, U., 2009. Evidence that light, carbon dioxide, and oxygen dependencies of leaf isoprene emission are driven by energy status in hybrid aspen. Plant Physiol. 151 (1), 448–460. https://doi.org/10.1104/pp.109.141978.

Rasulov, B., Talts, E., Bichele, I., Niinemets, Ü., 2018. Evidence that isoprene emission is not limited by cytosolic metabolites. Exogenous malate does not invert the reverse sensitivity of isoprene emission to high [CO_2]. Plant Physiol. 176 (2), 1573–1586. https://doi.org/10.1104/pp.17.01463.

Rodrigues, T.B., Baker, C.R., Walker, A.P., McDowell, N., Rogers, A., Higuchi, N., Chambers, J.Q., Jardine, K.J., 2020. Stimulation of isoprene emissions and electron transport rates as key mechanisms of thermal tolerance in the tropical species *Vismia guianensis*. Global Change Biol. 26 (10), 5928–5941. https://doi.org/10.1111/gcb.15213.

Rohmer, M., 1999. The discovery of a mevalonate-independent pathway for isoprenoid biosynthesis in bacteria, algae and higher plants. Nat. Prod. Rep. 16 (5), 565–574. https://doi.org/10.1039/A709175C.

Rosenstiel, T.N., Fisher, A.J., Fall, R., Monson, R.K., 2002. Differential accumulation of dimethylallyl diphosphate in leaves and needles of isoprene- and methylbutenol-emitting and nonemitting species. Plant Physiol. 129 (3), 1276–1284. https://doi.org/10.1104/pp.002717.

Sasaki, K., Ohara, K., Yazaki, K., 2005. Gene expression and characterization of isoprene synthase from *Populus alba*. FEBS (Fed. Eur. Biochem. Soc.) Lett. 579 (11), 2514–2518. https://doi.org/10.1016/j.febslet.2005.03.066.

Saunois, M., Stavert, A.R., Poulter, B., Bousquet, P., Canadell, J.G., Jackson, R.B., Raymond, P.A., Dlugokencky, E.J., Houweling, S., Patra, P.K., Ciais, P., Arora, V.K., Bastviken, D., Bergamaschi, P., Blake, D.R., Brailsford, G., Bruhwiler, L., Carlson, K. M., Carrol, M., Castaldi, S., Chandra, N., Crevoisier, C., Crill, P.M., Covey, K., Curry, C.L., Etiope, G., Frankenberg, C., Gedney, N., Hegglin, M.I., Höglund-Isaksson, L., Hugelius, G., Ishizawa, M., Ito, A., Janssens-Maenhout, G., Jensen, K.M., Joos, F., Kleinen, T., Krummel, P.B., Langenfelds, R.L., Laruelle, G.G., Liu, L., Machida, T., Maksyutov, S., McDonald, K.C., McNorton, J., Miller, P.A., Melton, J.R., Morino, I., Müller, J., Murguia-Flores, F., Naik, V., Niwa, Y., Noce, S., O'Doherty, S.,

Parker, R.J., Peng, C., Peng, S., Peters, G.P., Prigent, C., Prinn, R., Ramonet, M., Regnier, P., Riley, W.J., Rosentreter, J.A., Segers, A., Simpson, I.J., Shi, H., Smith, S. J., Steele, L.P., Thornton, B.F., Tian, H., Tohjima, Y., Tubiello, F.N., Tsuruta, A., Viovy, N., Voulgarakis, A., Weber, T.S., van Weele, M., van der Werf, G.R., Weiss, R. F., Worthy, D., Wunch, D., Yin, Y., Yoshida, Y., Zhang, W., Zhang, Z., Zhao, Y., Zheng, B., Zhu, Q., Zhu, Q., Zhuang, Q., 2020. The global methane budget 2000-2017. Earth Syst. Sci. Data 12 (3), 1561–1623. https://doi.org/10.5194/essd-12-1561-2020.

Schwender, J., Zeidler, J., Gröner, R., Müller, C., Focke, M., Braun, S., Lichtenthaler, F. W., Lichtenthaler, H.K., 1997. Incorporation of 1-deoxy-D-xylulose into isoprene and phytol by higher plants and algae. FEBS (Fed. Eur. Biochem. Soc.) Lett. 414, 129–134. https://doi.org/10.1016/S0014-5793(97)01002-8.

Sharkey, T.D., Loreto, F., 1993. Water stress, temperature, and light effects on the capacity for isoprene emission and photosynthesis of kudzu leaves. Oecologia 95 (3), 328–333. https://doi.org/10.1007/BF00320984.

Sharkey, T.D., 1996. Isoprene synthesis by plants and animals. Endeavour 20 (2), 74–78. https://doi.org/10.1016/0160-9327(96)10014-4.

Silver, G.M., Fall, R., 1991. Enzymatic synthesis of isoprene from dimethylallyl diphosphate in aspen leaf extracts. Plant Physiol. 97 (4), 1588–1591. https://doi.org/10.1104/pp.97.4.1588.

Sindelarova, K., Granier, C., Bouarar, I., Guenther, A., Tilmes, S., Stavrakou, T., Müller, J.-F., Kuhn, U., Stefani, P., Knorr, W., 2014. Global data set of biogenic VOC emissions calculated by the MEGAN model over the last 30 years. Atmos. Chem. Phys. 14 (17), 9317–9341. https://doi.org/10.5194/acp-14-9317-2014.

Siwko, M.E., Marrink, S.J., Vries, A.H., Kozubek, A., Uiterkamp, A.J., Mark, A.E., 2007. Does isoprene protect plant membranes from thermal shock? A molecular dynamics study. Biochim. Biophys. Acta Biomembr. 1768 (2), 198–206. https://doi.org/10.1016/j.bbamem.2006.09.023.

Spivakovsky, C.M., Logan, J.A., Montzka, S.A., Balkanski, Y.J., Foreman-Fowler, M., Jones, D.B.A., Horowitz, L.W., Fusco, A.C., Brenninkmeijer, C.A.M., Prather, M.J., Wofsy, S.C., McElroy, M.B., 2000. Three-dimensional climatological distribution of tropospheric OH: update and evaluation. J. Geophys. Res. 105 (D7), 8931–8980. https://doi.org/10.1029/1999JD901006.

Takada, M., Inoue, T., Mishima, Y., Fujita, H., Hirano, T., Fujimura, Y., 2012. Geographical assessment of factors for Sasa expansion in the sarobetsu mire, Japan. Journal of Landscape Ecology 5 (1), 58–71. https://doi.org/10.2478/v10285-012-0049-5.

Tani, A., Kawawata, Y., 2008. Isoprene emission from the major native *Quercus* spp. in Japan. Atmos. Environ. 42 (19), 4540–4550. https://doi.org/10.1016/j.atmosenv.2008.01.059.

Teng, A.P., Crounse, J.D., Wennberg, P.O., 2017. Isoprene peroxy radical dynamics. Journal of the. American Chemical Society 139 (15), 5367–5377. https://doi.org/10.1021/jacs.6b12838.

Tingey, D.T., Manning, M., Grothaus, L.C., Burns, W.F., 1979. The influence of light and temperature on isoprene emission rates from live oak. Physiol. Plantarum 47 (2), 112–118. https://doi.org/10.1111/j.1399-3054.1979.tb03200.x.

Torii, A., 2003. Bamboo forests as invaders to surrounded secondary forests. J. Jpn. Soc. Reveg. Technol. 28, 412–416.

Vickers, C.E., Possell, M., Laothawornkitul, J., Ryan, A.C., Hewitt, C.N., Mullineaux, P. M., 2011. Isoprene synthesis in plants: lessons from a transgenic tobacco model. Plant Cell Environ. 34 (6), 1043–1053. https://doi.org/10.1111/j.1365-3040.2011.02303.x.

Way, D.A., Schnitzler, J.P., Monson, R.K., Jackson, R.B., 2011. Enhanced isoprene-related tolerance of heat- and light-stressed photosynthesis at low, but not high, CO_2 concentrations. Oecologia 166 (1), 273–282. https://doi.org/10.1007/s00442-011-1947-7.

Wiberley, A.E., Donohue, A.R., Westphal, M.M., Sharkey, T.D., 2009. Regulation of isoprene emission from poplar leaves throughout a day. Plant Cell Environ. 32 (7), 939–947. https://doi.org/10.1111/j.1365-3040.2009.01980.x.

Wildermuth, M.C., Fall, R., 1996. Light-dependent isoprene emission (characterization of a thylakoid-bound isoprene synthase in *Salix* discolor chloroplasts). Plant Physiol. 112 (1), 171–182. https://doi.org/10.1104/pp.112.1.171.

Wildermuth, M.C., Fall, R., 1998. Biochemical characterization of stromal and thylakoid-bound isoforms of isoprene synthase in willow leaves. Plant Physiol. 116 (3), 1111–1123. https://doi.org/10.1104/pp.116.3.11.